

# Messengers: Breaking Echo Chambers in Collective Opinion Dynamics with Homophily

Mohsen Raoufi<sup>1,2,3\*</sup>, Heiko Hamann<sup>1,4</sup> and Pawel Romanczuk<sup>1,2</sup>

<sup>1</sup>Science of Intelligence, Research Cluster of Excellence, Marchstr. 23, Berlin, 10587, Germany.

<sup>2</sup>Department of Electrical Engineering and Computer Science, Technical University of Berlin, Marchstr. 23, Berlin, 10587, Germany.

<sup>3</sup>Department of Biology, Humboldt University of Berlin, Philippstr. 13, Berlin, 10115, Germany.

<sup>4</sup>Department of Computer and Information Science, University of Konstanz, Box 188, Konstanz, 78457, Germany.

\*Corresponding author(s). E-mail(s): [mohsenraoufi@icloud.com](mailto:mohsenraoufi@icloud.com);

Contributing authors: [heiko.hamann@uni-konstanz.de](mailto:heiko.hamann@uni-konstanz.de);

[pawel.romanczuk@hu-berlin.de](mailto:pawel.romanczuk@hu-berlin.de);

## Abstract

Collective estimation manifests computational intelligence emerging from inter-individual local interactions, e.g., by aggregating opinions from neighbors to estimate a quantity. Use cases of collective estimation may include directed motion in physical space, such that agents, for example, have to collectively explore a distributed feature, and collectively agree on a numerical value. In doing so, collectives face several challenges in achieving precise estimations. These challenges exhibit complex behaviors, particularly when the interaction network and opinion of agents evolve simultaneously. We take homophilic networks as an example, where disproportionate interaction with like-minded neighbors leads to the emergence of echo chambers, preventing collective consensus. Our simulation results confirm that, besides a lack of exposure to attitude-challenging opinions, seeking reaffirming information entraps agents in echo chambers. We propose a generic novel approach based on a Dichotomous Markov Process (DMP) where stubborn agents (called Messengers) connect the disconnected clusters by physically transporting their opinions to other clusters to inform and direct the other agents. We show that diverse collective behaviors arise from the DMP and study a continuum between task specialization with no switching (full-time Messengers), generalization with slow task switching (part-time Messengers), and rapid task switching (short-time Messengers) and its impact on system

performance. Our results show that stubborn agents can, in various ways, break the echo chambers and promote consensus in collective opinion.

**Keywords:** Opinion Dynamics, Collective Estimation, Homophily, Echo chambers, Dichotomous Markov Process

## 1 Introduction

Collective behaviors exhibited by animal collectives or groups of interacting artificial agents are fascinating examples of self-organization. They enable groups to solve problems collectively, that cannot be solved by any individual alone. This phenomenon is often referred to as collective or swarm intelligence [1–3]. While significant progress has been made over the past decades in understanding the fundamentals of collective intelligence, many questions remain open regarding actual mechanisms underlying collectively intelligent behavior, in particular in spatially embedded systems lacking the capability for global information exchange between individual agents.

Among the many different exhibitions of intelligence in collectives, the wisdom of crowds effect [4–6] stands out as a great candidate for studying collective computational intelligence [3]. While the core idea—that the average of many imperfect estimations can be remarkably close to the true value—seems straightforward, achieving wise and precise estimations depends on meeting certain criteria [5, 7–10]. Typically, it assumes full knowledge and all estimations are fully accessible, which is not naturally feasible in decentralized settings. However, distributed consensus models, particularly DeGroot-like models [11], implement the wisdom of crowds effect without a centralization assumption [7, 12]. These models also provide mechanisms for how opinions spread across the interaction network, leading to behaviors known as opinion dynamics [13, 14]. Achieving a consensus has shown potential applications in collective estimation scenarios and can be used in a variety of engineering fields ranging from machine learning to networks of sensors and groups of robots [15–17]. Moreover, studying these behaviors gives insights into how similar complex systems work, as used in economics, politics, and social sciences [7, 14, 18–20]. Modeling behavior on the individual level helps in explaining the dynamics of opinion spread in collectives. These models usually follow a very simple set of rules; Examples are Voter models, bounded confidence, and gossip methods [21–23]. The underlying network of interaction among agents is an important determinant of collective behavior [23, 24]. For example, we know that the connectivity of the network controls the tradeoff between speed and accuracy of consensus formation in collectives with static interaction networks—stronger connected networks promote faster consensus decisions at the expense of decision accuracy [10, 17].

### 1.1 Homophily and Echo Chambers

Contrary to the assumption of static networks in early models of opinion dynamics, many systems display dynamic networks, as agents tend to constantly rearrange their connections with their peers, making the collective behavior more complex [25]. These rearrangements can be described following different rules specifically defined for the network dynamics; for

instance, consider homophily: the disproportional tendency of agents to establish links with like-minded neighbors [26–28]. By adding a new dynamic to the interactions, and hence altering how the information flows in the network, homophily changes the resulting collective behavior. One consequence of homophily in network dynamics is the emergence of “echo chambers”: clusters that are highly homogeneous internally and very heterogeneous compared to each other. The strong effects of homophily and echo chambers on collectives highlight their critical importance; particularly, when these effects lead to the emergence of phenomena that are considered threats to human society [29]. For instance, their effect on the spread of misinformation [30, 31], where the homogeneity of information within clusters acts as a driver to the diffusion of misinformation [29, 32, 33]. Ultimately, echo chambers reinforce only the existing perspective, foster confirmation biases, and prevent clusters from receiving attitude-challenging information [30, 32, 34]. Other consequences of homophily include the formation of filter bubbles and network segregation [19, 33]. Despite their adverse effects at the collective level, these echo chambers function for a purpose on the individual level: comforting agents with reaffirmation and protecting them from disagreement [32]. Although the actual adversarial outcome of echo chambers in collective dynamics is arguable [35], they indeed inhibit the flow of information on the network in our scenario where achieving consensus is an objective.

## 1.2 Scenario: Embedded in Space and Online Sampling of Information

We introduce a novel scenario that pushes towards a physical embedding of opinion dynamics as it would be the reality for a group of mobile agents. We updated our opinion dynamic model to embed information in space. Many models have already been developed to describe a mechanistic process of how the co-evolution of homophilic networks and opinion dynamics lead to the emergence of echo chambers and complex collective behavior [36–38]. Although the opinion updating models used parallel to the network dynamics vary greatly in the literature, they presume that the initial opinions of agents come from a random pool of possible (discrete) options. Hence, these models did not focus on the origin of the opinions, but rather their evolution through social interactions. Furthermore, this elimination of information sources is inevitably reflected in the opinion-updating model, as its influence on the evolution of opinion is not further considered. Contrarily, we assume that the information agents receive comes from a specific source, and the agent’s position determines the information available to them, hence shaping their opinion. We already know that the position of agents in the network matters [39], but so does the position with respect to the information source. Therefore, we add the information space in our model to account for its effects on shaping opinions. This space resembles the source of information available to agents and is modeled as a 2D Euclidian space, similar to our previous work [17]. Compared to the previous discrete models of initial opinions in homophilic networks, the information landscape provides continuous opinions with arbitrary distributions *throughout* simulations.

## 1.3 A Motion Model: Homophily as a Pulling Force

Given our agents are embedded in an information space, we require new rules to implement homophily in space. Similarly, we define neighborhood as the local proximity (determined by

communication range) of agents in the information landscape. This definition of communication range compares to the thresholds in bounded confidence models of opinion dynamics [22, 40]. In the original models of homophily without spatial constraints on network assumptions, homophily could affect links between any two random nodes, regardless of their spatial position [36]. In a spatial network, however, homophily needs to be redefined concerning space. Therefore, we propose a potential function based on the dissonance value of agents’ opinions, where homophily acts as a gravitational pulling force. Homophilic agents actively move and seek sources of information that optimize this value to a minimal disagreement. This way of modeling homophily is in line with the aforementioned functional purpose of homophily–reducing disagreement [32]. We later argue that this definition relates to the minimum surprise principle. As we showed in our previous work [41], the spatial embedding of information and spatial network is reflected in the collective pattern formation. The result in space is an emerging complex collective behavior, called contour-capturing. Compared to the non-spatial models, echo chambers did not emerge unconditionally in the specific settings of our previous work.

#### 1.4 Our Approach: Messengers

To address the problem of echo chambers in our specific scenario, we introduce a new concept of ‘Messengers.’ They are allowed to cross the information space without sampling and serve as data ferries to virtually connect sub-populations across wider distances beyond the communication range limits. In non-spatial networks, a significant parameter in promoting the formation of echo chambers is the limited access of agents to attitude-challenging information [30], i.e. information that deviates from the current belief of the agent. In our model with spatial networks, reducing the communication range would leave the same effect. In this paper, we study how a limited communication range leads to the emergence of echo chambers, in our spatial scenario. Our results confirm that homophily indeed hinders the flow of information, and prevents the collective from achieving a global consensus. To get out of the local optimal trap of echo chambers, agents need to receive diverse opinions flowing into their homogeneous clusters. It might be achieved when agents can communicate with neighbors out of their filter bubble or can escape from the pull of homophily. Thus, as a solution, we define a new state for agents, called Messenger, where they could move freely in space and

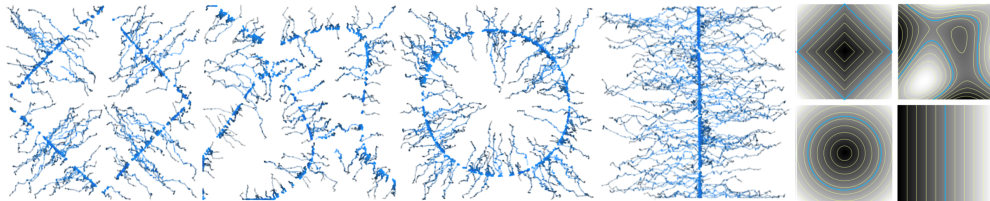


**Fig. 1:** Collective contour capturing emerges as the result of collective opinion dynamics and homophily in space. The traces of agents start with black and become blue (and brighter) over time. Agents converge from the initial random distribution to the mean contour lines of the environment for four different information landscapes. Each plot on the left side corresponds to an information distribution on the right gray scale plot, with the iso-contour lines shown in light yellow and the mean contour line (ground truth) in thick blue line.



share their information with others. We investigate if this solution can potentially increase the effective communication range and bring the consensus back to the collective. A challenge, however, is to have a decentralized mechanism for agents to decide whether, when and for how long agents should take a state, and then follow the behavior rules accordingly. Here, we propose and describe a simple decentralized solution based on the Dichotomous Markov Process (DMP) [42]. We study the effect of DMP parameters on individual and collective behaviors, measured by two properties: the ratio of Messengers, and the switching speed between the two states. We then explore the phase diagram of collective behavior and elaborate on an example of collective behavior at each phase. In addition, we highlight a tradeoff between the generalization against specialization of agents and a tradeoff on the population share of Messengers in the collective.

## 2 Results

In this section, we investigate the complex behavior of collective consensus resulting from the interplay between opinion dynamics, originating from conformity, and homophily, which is modeled by the movement of agents in space. We then study the emergence of echo chambers in low connectivity regimes and explore a potential solution to restore consensus based on the introduction of an additional state of individuals, which we refer to as Messenger, and a Dichotomous Markov Process (DMP) governing the stochastic transitions between the ordinary state of socially interacting agents and messengers.

### 2.1 From Consensus to Dissensus in Space: The Emergence of Echo Chambers

As shown previously in [41], the coupling of the local information aggregation and homophily not only allows agents to estimate the mean value of information distribution in the environment but also leads to an emergent spatial collective formation in the physical space (see Fig. 1), referred to as collective contour-capturing behavior. The resulting patterns show that in seeking specific information sources, individuals actively move in space, and collectives form communities based on the information they receive. Here, we explore the result of such complex behavior in more detail and show that global convergence relies on a sufficiently large communication range. In settings with limited connectivity, however, a breakdown to only a local consensus is observed. The result of limited connectivity and homophily is that the system becomes trapped into local minima, leading to the formation of echo chambers, with negative consequences on the collective performance due to the inhibition of information flow across the clusters with dissimilar opinions (see Fig. 2).

Additionally, the results demonstrate that echo chambers block the collective movement and prevent it from achieving a consensus in space, i.e. the collective contour-capturing. The clusters emerging from the social interaction model we present in Sec. 4.1 exhibit spatial properties that are otherwise overlooked. An example of such cluster formation is shown in Fig. 3-a, where the echo chambers appear as concentric arcs of various radii, in this case for radial information distribution. In general, the echo chambers take *parallel* forms which are also parallel to the iso-contours of the information landscape.

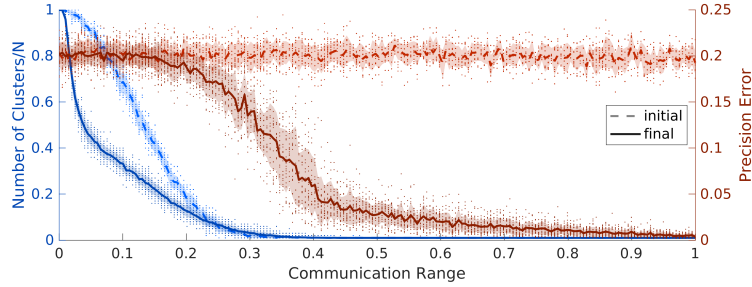


**Fig. 2:** Normalized number of clusters and opinion precision error decrease by communication range at the beginning and end of simulations for the baseline setup.

Although the original method demonstrated the ability to achieve the contour capturing performance in different environments [41], it is limited to collectives with sufficient connectivity. To show this, we considered the precision of consensus as well as the number of clusters being formed at the end of the experiment. A consensus *in space* is achieved when agents are precisely on the same contour line. We illustrate these two metrics in Fig. 2, with the number of clusters and spatial precision error ( $E_p^S$ , for further information, see Sec. 4.4.) The number of clusters and precision error decrease with the communication range after a critical value ( $r_{\text{comm}} \approx 0.3$ ), highlighting a specific regime where the consensus breaks due to the lack of connectivity. This critical value is the minimum required for the initial network to be fully connected. By comparing the final and initial state of the collective in Fig. 2, we argue that the basic method still enhances both the cohesion and precision of the collective. However, in the collectives with very low connectivity, e.g.  $r_{\text{comm}} = 0.1$ , the precision is diminished. We propose and investigate a solution in the next sections to increase effective connectivity by utilizing information-carrying mobile agents, termed ‘Messengers’. The agents switch between the two states following the DMP, which we examine in the following section.

## 2.2 Dichotomous Markov Process as a State Switching Mechanism

The solution we propose in this paper is based on the switching mechanism of the DMP, defined by the two parameters  $p_M$  and  $p_E$ . Fig. 4-a illustrates the time history of a single agent’s state. Changing the parameter pair influences two properties of a single agent behavior: the ratio of time each agent spends in either of the two states; and how quickly they switch between the two states. The latter, known as the sojourn time (see Sec 4.3), refers to the time between two consecutive switches. We illustrate the second time spent in the Exploiter and Messenger states in Fig. 4-a by  $\tau_M^2$  and  $\tau_E^2$ , respectively. At the collective level, changing the two parameters affects the collective average sojourn time ( $\tau_S$ ), and the ratio of Messengers ( $m$ ). These two properties are depicted in the 2D parameter space in Fig. 4-b, c.

We evaluated the Markov process by running multiple independent Monte-Carlo simulations and validated it by comparing the numerical results with the analytical properties in Eq. 7, and 8. The result of analytical and numerical simulations in Fig. 4-b, c suggests validation of the numerical simulation. The switching speed reaches its maximum in the top-right corner of the parameter space ( $\log_{10} p_E \approx 0$ ,  $\log_{10} p_M \approx 0$ , see Fig. 4-b) and decreases

toward the bottom-left corner (small values of  $p_E$  and  $p_M$ ). In the top-left corner of Fig. 4-c, the collective is mainly comprised of the Messengers and the ratio decays diagonally to the bottom-right corner. For the sake of comparison, in the rest of the paper, we refer to the setup without Messengers as the *baseline* setup. In the following sections, we explain how these two properties determine the collective performance. We evaluate the performance of the collective for different DMP parameters in two terms: consensus in the opinion domain, and consensus in space, i.e. contour-capturing behavior.

### 2.3 Opinion Consensus with Messengers

In order to prevent the system from fragmenting into isolated opinion clusters, i.e. echo chambers, we extend the model by introducing a Messenger state. In this state, each agent behaves as data moving randomly in space. Messengers can make the information propagate and spread beyond the limitation of the communication range. A key outcome of introducing Messengers is the achievement of opinion consensus even in low connectivity regimes, which was previously impossible. However, this also introduces a new dimension to the problem: deciding which behavior agents should follow. As we explain in Sec. 4.1, agents switch between the two behaviors following a DMP. Here, we study how the two main parameters of the DMP ( $p_M$  and  $p_E$ ), the transition probabilities, modulate the collective performance in terms of opinion consensus.

We illustrate the normalized opinion precision error ( $E_p^O$ ) across the parameter space in Fig. 5. Each point in the 2D space of  $p_M$  and  $p_E$  represents a pair of parameters corresponding to a specific configuration for the DMP. The bottom-right corner point is analogous to the baseline setup, where the ratio of Messengers is zero. This serves as our reference for normalization, with each point's normalized performance being the ratio of its absolute

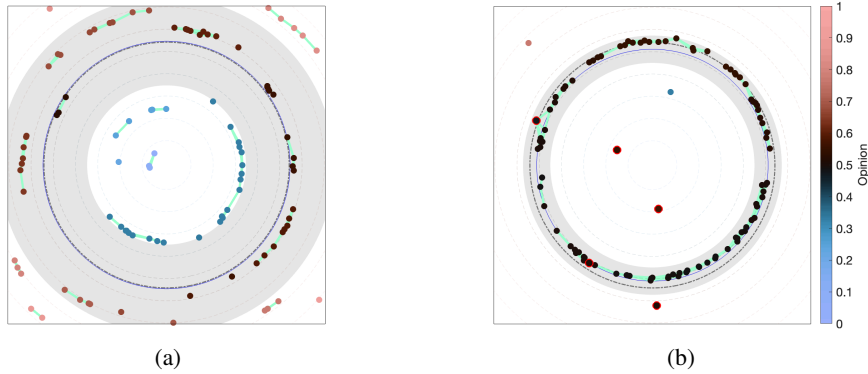
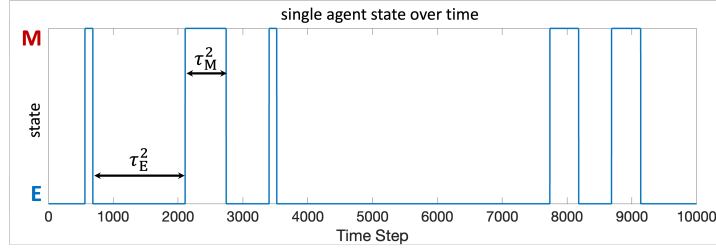
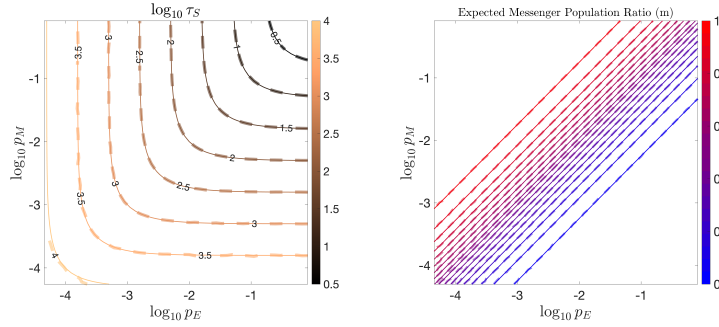


**Fig. 3:** Final position of agents in the information landscape. a) Formation of echo chambers due to limited connectivity and homophily (baseline setup), b) consensus is achieved by introducing Messengers (with red circles around them). The fill-in colors correspond to the opinion agents have, the green lines show the links of the communication network, and the width of the gray ring shade indicates the spatial precision error. The dashed gray rings and the blue ring show the contours of the information distribution, and the contour related to the mean value of the collective, respectively.



(a)



(b)

(c)

**Fig. 4:** Changing the pair parameters of the DMP affects the individual and collective properties. a) An example realization of the DMP with  $p_E = 0.003$ ,  $p_M = 0.0004$ , showing the time history of a single agent state switching between Exploiter (E) and Messenger (M) states determined by the Markov process. The time duration of staying in either of the states in the 2<sup>nd</sup> sojourn is denoted by  $\tau_E^2$  and  $\tau_M^2$ . b) Average sojourn time of the DMP, and c) the ratio of Messenger population shown with 5 percent intervals for the analytical and numerical simulations with solid and dashed lines respectively.

performance to that of the baseline. The figure shows that the baseline setup (bottom-right corner), where all agents are Exploiters, is not optimal. The higher performance of other regions indicates that introducing the Messengers can promote the consensus of opinions. Also, the collective performance is a significant function of the DMP parameters. Changing the parameters can move the system across different regimes, with certain configurations being locally optimal. Identifying these local optimal regions will aid in understanding the conditions necessary for achieving consensus, and provide guidelines for designing such systems. For ease of reference, we marked the parameter space with specific regions of qualitatively similar behavior.

According to the properties of the DMP (see Sec. 4.3), the bottom and left parts of the parameter space correspond to the regions with slow switching (large  $\tau_S$ ) of states on average, with agents remaining in at least one of the states for very long times. Given that agents in these regions rarely switch their states (see Fig. 4-b), we can consider them as *specialized* individuals. This is in contrast to the top-right corner, where *generalized* agents frequently

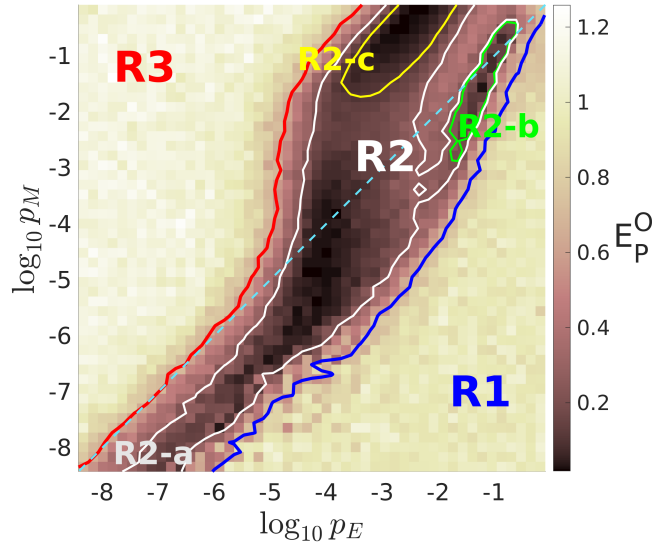


**Fig. 5:** Normalized opinion precision error w.r.t the baseline setup indicating different areas in the parameter space. R1: Too few Messengers (too greedy); R2: Set of regions with a balanced number of Exploiters and Messengers, R2-a (Specialized Exploiters): Specialized slow-switching agents with Exploiters in the majority, R2-b (Enhanced Exploration): Fast-switching agents, R2-c (Generalized Messengers): Majority being fast-switching Messengers; R3: Too many Messengers. The supplementary video of the simulations for a sample of each region is available via this link: <https://figshare.com/s/61052656b78288a5fb47>.

switch between the two states, corresponding to short sojourn times. The generalized agents experience both states during the course of the experiment. Additionally, if we divide the space off-diagonally into two triangles, the lower right triangle predominates with Exploiters. We already know that the ratio of Messenger population decreases from the top-left to the bottom-right corner of the parameter space (see Fig. 4-c.)

### 2.3.1 Integration-vs-Information Tradeoff

In Fig. 5, as we go up diagonally from the bottom-right corner to the upper-left corner, we encounter collectives with varying proportions of Exploiters. For instance, in region R1, Exploiters constitute the largest share of the population on average resulting in overly clustered collectives, where agents immediately entrap to the local echo chambers. The opinion consensus performance in this region is deficient due to the prevalence of many greedy Exploiters. We consider an Exploiter as an integrator of information by processing it following the social learning DeGroot model (see Sec. 4.1.) Therefore, R1 is dominated by agents acting as an *integrator* of the available information. Their greedy and exploitative behavior prevents the flow of new information across clusters. In this setting, the system exhibits the most conservative behavior in terms of mobility and tends to over-exploit in terms of information aggregation. For engineering applications, especially where moving is costly or

hazardous, selecting parameters closer to this region might be preferred. Conversely, R3 represents an overly spread region where extreme exploration of Messengers and inadequate processing of available information negatively impact performance. In this region, Messengers, acting as moving *information*, are redundant; while there are insufficient Exploiters to integrate their information into the collective. In R3, collectives demonstrate the highest network plasticity, meaning any two random agents are likely to meet each other, irrespective of their opinions. R1 and R3 are extremes of either exploitation or exploration, respectively. The high-performing regions are situated between these two extremes, closer to the off-diagonal line (the blue dashed line). We labeled this *balanced* region as R2. This region contains all local optimal regions between the blue and red contours. Next, we examine different locally optimal regions within R2, focusing on varying switching timescales.

### 2.3.2 Generalization-vs-Specialization Tradeoff

We know that moving from the bottom-left to the top-right corner of the parameter space decreases the timescale (increases the frequency) of switching between the two states, as shown in Fig. 4-b. This change in the DMP timescale influences the optimal regions within R2. Near the bottom-left corner, R2-a is located below the off-diagonal line. The corner represents *specialized* agents who do not switch their state during the simulation and maintain their initial Exploiter or Messenger states. The tail of R2-a aligns with the iso-lines of Messenger ratios (see Fig. 4-c). This indicates that the system requires a specific ratio of Messengers that is significantly less than half. Accelerating the switching frequency (towards the top-right) increases the likelihood of agents experiencing both states, thus making them more *generalized*. As we go up in this space, the high-performing points gradually shift towards higher Messenger ratios near the center of the parameter space. This pattern suggests that, on average, more Messengers are needed in generalized collectives compared to the specialized ones. Increasing the switching frequency further results in the branching of R2 into two distinct sub-regions: R2-b and R2-c.

R2-b, the lower branch of this fast-switching region, is not parallel to the iso-lines of  $m$  (Messenger ratio). This implies that the optimality of R2-b is caused by both properties of the DMP. In this region, the points below the off-diagonal line (lower  $m$ ) are associated with longer timescales. Whereas points with higher Messenger ratios (above the line) favor faster switching. Longer timescales for Messengers mean that they have more time to transport the information they carry, effectively lengthening the link they create. However, compared to R2-a, Messengers in R2-b do not traverse for long durations. Consequently, R2-b is an optimal region, especially in scenarios where movement and exploration incur significant costs. Observations of agents' behavior during simulations (see the Supplementary material) reveal that this configuration enhances the collective's exploration behavior. Unlike R2-b, R2-c comprises a majority of Messengers and is elongated parallel to the iso-lines of Messenger ratios. This pattern suggests that the optimal parameter configurations in R2-c primary depend on  $m$ , and are not strongly correlated with  $\tau_s$ . This region is distinguished by effective information mixing, promoted by the abundance of Messengers moving randomly in space. The slower configurations outside of R2-c are less optimal, as Messengers transport information across longer distances than necessary. The superiority of faster dynamics in this region underscores the significance of spatio-temporal coupling in the problem. We later show that, compared to R2-b, convergence is achieved more rapidly in the R2-c region (see Fig. 6.)

### 2.3.3 Temporal Evolution of Parameter Space

By examining snapshots of the parameter space at different time steps, we obtain insights into the temporal evolution of the various regimes in the parameter space. Observing the system’s progression over time helps us to track the emergence and development of each of the optimal regions (as shown in Fig. 6). This approach enables a comparison of the temporal characteristics of each region and allows us to evaluate their performance in scenarios with different time budgets available for the overall task. For instance, the high-performing optimal region located at the bottom-left of the space demonstrates consistent performance, irrespective of the time limit. It maintains its optimality across all time limits, suggesting a more robust and reliable performance. This region is characterized by agents that are *specialized* in their initial states. The gradual slight diagonal shift of this region’s tail to the lower right, observable from Fig. 6-a to e, indicates that a lower (specialized) Messenger ratio is favorable in scenarios with longer time budgets.

In contrast, the generalized Exploiters, located in the top right narrow valley (R2-b), emerge only when the system has enough time to process the task. It is important to note that this region is advantageous as it minimizes precision error in both the physical and opinion domains, as we discussed in Sec. 2.4. Additionally, we observe a bifurcation in the fast-switching parameter regime. Specifically, the small head of the elongated R2 (see Fig. 6-b) grows over time and eventually branches into two distinct regions (R2-b and R2-c). The gap between the two branches widens over time. Another notable temporal shift occurs in the generalized Messenger region, the larger upper left branch (R2-c) by gradually ascending toward higher Messenger ratios. This suggests that in scenarios with higher time budgets, increasing exploration efforts—by assigning more agents to perform random walks—is advantageous. The final aspect to highlight is the continual improvement in the precision of the optimal regions. The gained precision over time underlines a speed-accuracy tradeoff in this scenario. In contrast, the extreme parameter setups, such as those characterized by excessive exploitation or randomness (R1 and R3), do not exhibit any significant improvement over time.

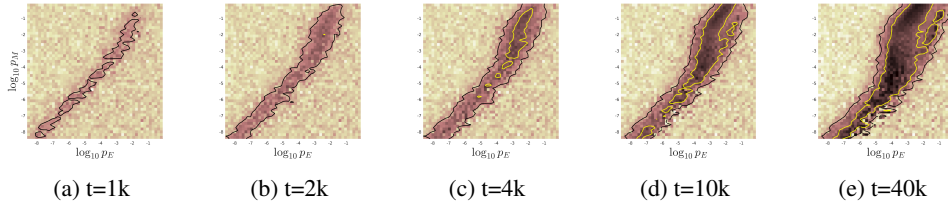


**Fig. 6:** Time development of parameter space for precision error. Bifurcation of the optimal parameters happens for the top-right side of the parameter regime corresponding to fast dynamics, while the bottom-left corner does not undergo a significant shift, showing a more robust performance by the time limit.



## 2.4 Contour Capturing Performance

We turn now to evaluating the precision error in the spatial domain, measured by  $E_P^S$ . This metric quantifies the collective performance in contour-capturing tasks and is particularly useful when access to the internal opinion of agents is not feasible. The results, as depicted in Fig. 7-a or b, do not offer any additional high-performing regions compared to those already identified in Fig. 5. However, the local optimal regions above the diagonal disappear. This is because excessive random walks by too many Messengers do not contribute to spatial convergence. The difference between the two metrics,  $E_P^S$  and  $E_P^O$ , signifies that while consensus may be achieved in the opinion domain, it does not necessarily translate to a spatial consensus.

Unlike opinion consensus, successful contour capturing requires agents to be more conservative. Indeed, the random movement of an excessive number of Messengers in space increases the system's spatial precision error. Similar to the findings in opinion consensus, the same narrow optimal region representing generalized Exploiters (similar to R2-b in Fig. 5), and the long tail characterizing specialized Exploiters (comparable to R2-a) are again identified as high-performing regions in terms of spatial consensus. This observation suggests that converging on similar sources of information promotes the achievement of opinion consensus, but not necessarily vice versa.

### 2.4.1 The Effect of Initial State Distribution of the DMP

We already have established that the temporal properties of the DMP significantly affect collective performance. Another important aspect to consider is the distinction between the system's transient and stationary behaviors. Up to this point, we have assumed that the DMP begins with the expected analytical ratio of Messengers, thereby initially placing the process in its stationary state. However, any deviation from this stationary state puts the system into a transient phase. The progression towards reaching the stationary state is time-dependent and the transient behavior of the DMP also influences the collective performance. Specifically, we show that the transient behavior is linked to the DMP relaxation time ( $\tau_C$ ) [42] (see

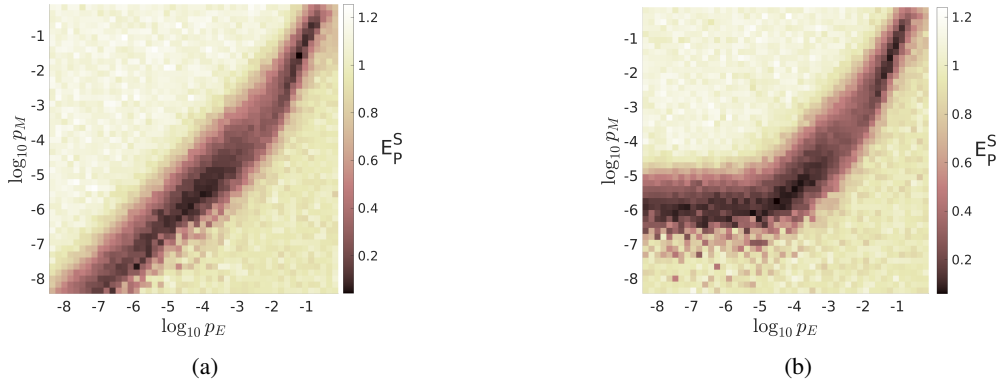


**Fig. 7:** Normalized spatial precision error for different parameters of the DMP. The effect of the initial number of Messengers on the contour capturing performance for a) initial state with the expected number of Messengers, b) initial state without any Messengers.

Fig. 10 in the appendix). Next, we will explore how the system’s behavior is affected by its initial condition, particularly focusing on the initial population of Messengers. To show this difference in Fig. 7, we conduct a comparison to a case where the system starts without any Messengers. We know that, given fixed transition rates, the system requires time to attain the expected analytical stationary properties, namely the Messenger population ratio.

The observed differences are particularly noticeable in DMPs with large timescales (bottom-left corner in Fig. 7). A comparison of the two figures shows that for slow-switching dynamics, the tail of the optimal region bends upward under non-stationary initial conditions. This suggests that the absence of initial Messengers is compensated for with higher  $p_M$  values. In such scenarios, the actual average Messenger ratio falls below its expected stationary value due to the transient behavior of the Markov process.

Same as the temporal development studied earlier in Fig. 6, by comparing the parameter space at different time steps we observe that systems with different time-scales reach their stationary state with different speeds. For example, systems with fast-switching dynamics in the top-right corner reach their stationary states more quickly, which makes them more robust to varying initial conditions within the same time constraints. In contrast, slower systems require more time to gradually approach their stationary states. Consequently, we observe that the horizontal tail of R2 shifts downward, eventually aligning with a shape similar to that depicted in Fig. 6-a. With these observations, we highlight the importance of accounting for transition effects, particularly in scenarios where the properties of the system must dynamically change from one configuration to another. They also provide insights for engineers in designing robust systems against variations of initial conditions and selecting parameters from different optimal regions.

## 2.4.2 Different Information Distributions

Our main focus in this paper is on the specific case where the spatial distribution of the information is radial, i.e. the iso-contour lines form circular shapes. This configuration resembles a range of natural situations where a point-like source isometrically emits a concentration into its surroundings, which may then spread through processes like diffusion or convection. To ensure generality, we also tested our model’s performance in environments with various other distributions. The first row of Fig. 8 presents different information distributions, where agents (depicted as cyan dots) converge to the zero-bias (ground-truth) contour line (indicated by a red dashed line). The introduction of Messenger with tuned DMP parameters shows an improved performance across all four environmental benchmarks.

In the second row of Fig. 8, we present the optimal regions within the parameter space for different information distributions. While the shape of these optimal regions varies slightly depending on the distribution, the principles and the arguments discussed in other subsections of the paper remain applicable to each of them. For this subsection, we restricted our analysis to the top-right quarter of the previously broader parameter space, since the most non-trivial optimal regions are located in this quarter. Furthermore, we selected a specific optimal parameter pair (marked with the green dot) to demonstrate the final agent spatial distribution for this particular DMP configuration. This visualization confirms that the chosen parameter set results in a satisfactory spatial consensus across all tested information distributions. Additionally, we adapt our model to an abstract 1-dimensional environment, with a few modifications,

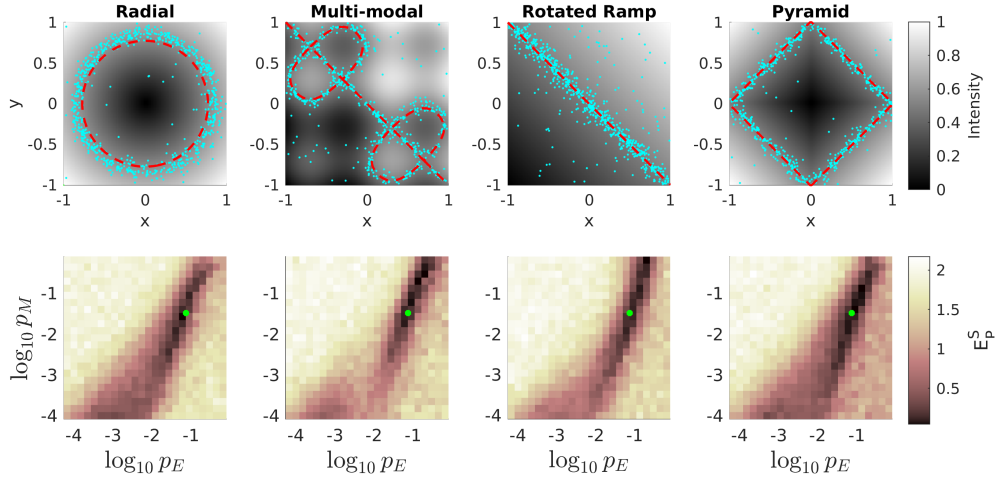


**Fig. 8:** The performance of the collective in different environment distributions. First row) the information distribution in space, and its mean contour line (red dashed line). The cyan dots show the scattered position of agents at the end of each simulation for the specific parameter marked by the green dot in the respective figure in the second row. Second row) the precision error ( $E_p^S$ ) for the corresponding environment.

such as the implementation of random walk (see appendix). The outcomes from this setting show only negligible qualitative differences compared to the 2D environment.

### 3 Discussion

The integration of explicit spatial behavior into the collective opinion dynamics model introduces a new dimension to the complexity of the model. We demonstrated this through several components: a) initializing opinions based on spatial distribution, b) defining the interaction network according to spatial local proximity, and c) driving agents' movement in space through homophily. The interplay of these elements results in complex collective behavior, where homophily in space leads to emergent patterns that match with the spatial distribution of information, the so-called 'contour capturing behavior.' We interpret this collective pattern formation as a type of spatial consensus and show that the consensus on the pattern is conditional on having sufficient network connectivity. Our simulations for collectives with low connectivity indicate that the greedy behavior of agents leads to the collective becoming trapped in local optima, a process we associate with the emergence of echo chambers. A unique feature of these echo chambers is their similar shapes, which mirror the spatial information distribution. The spatial patterns constructed by the echo chambers reflect the properties of the information landscape and are a consequence of the spatial dynamics of the system, typically ignored in opinion formation models. Also, our findings indicate that these echo chambers inhibit the flow of information, which prevents the collective's ability to reach a precise consensus. It is important to clarify that the impact of network connectivity is relative to the size of agents' distribution. Low connectivity can stem from either a limited communication range or an extensive initial diversity in opinion space. This observation

highlights a potential disadvantage of excessive opinion diversity in a collective when the communication range is limited.

We suggested that a method to overcome the local traps inherent in low-connectivity networks is to indirectly extend the effective communication range. This is particularly relevant in systems comprising mobile agents. By leveraging mobility and employing certain individuals as embodied data carriers, individuals can interact beyond the physical limits of their communication. To this end, we introduce a new behavioral role for agents, the *Messenger* state. This state allows designated agents to function exclusively as carriers of information. A Messenger is a stubborn agent with a fixed opinion, sharing its opinion while moving randomly in space. These agents can be viewed as links to the history of opinions of agents, with their independent random movement promoting broader exploration. Yet, defining a new state for agents poses a new challenge: determining how agents should select their state. To address this challenge, we employed the Dichotomous Markov Process (DMP) as a distributed switching mechanism for agents to switch between behaviors. DMP gives agents a mechanism to decide at each time step whether they should switch to the other state or stay in their current state. A key advantage of this approach is its decentralization and scalability.

Still, the two parameters of the DMP add a dimension of freedom to the problem that requires consideration. Modifying the DMP parameters directly determines the temporal properties of the switching mechanism for a single agent. This, in turn, indirectly modifies the collective’s properties, such as the ratio of Messengers and the speed of switching (denoted as  $m$ , and  $\tau_S$ ). The expected value of these two properties can be described analytically as a function of the DMP parameters. We used these analytical values to validate the implementation of the Markov process in our numerical simulations. We showed that these properties significantly influence the collective performance, in achieving consensus in both the opinion and space domains.

Our numerical results mark several local optimal regions where the collective achieves the highest precision in consensus, which is the ultimate objective in this scenario. Each region exhibits unique characteristics, reflecting a spectrum of collective behaviors derived from the DMP. We distinguished these regions based on the two key properties of the DMP. The high-performing regions for achieving consensus vary depending on the consensus domain—opinion or spatial—used to evaluate the system. By adjusting the DMP parameters, agents can adapt their performance and navigate the various tradeoffs we have identified. We elaborate on some of these tradeoffs such as information versus integration, and generalization versus specialization. Generally, extremes in the number of Messengers—either too few or too many—prove suboptimal. Pushing the system towards them results in either excessive exploitation and greedy behavior or randomness and chaos. The high-performing settings were located in the middle ground. We have categorized these regions into three distinct groups, each distinguished by the switching frequency of the DMP.

The range of switching frequency spans from no switching to excessively fast switching. Agents at these extremes are identified as being specialized or generalized, respectively. Compared to the Messengers ratio, the dimension of switching frequency introduces a more nuanced trade-off, as we elaborated in the Results section. We found that even a minimal number of Messengers can reestablish consensus in collectives when agents maintain fixed states throughout the simulation—being specialized. On the other hand, faster switching can result in two distinct high-performing behaviors: improved exploration for lower Messenger

ratios; or conservation of information for higher Messenger ratios and updating the opinions only rarely. In the former, the fast-switching Messengers perform random walks long enough to help the collective escape the local optima of echo chambers. The latter is the case for collectives mainly composed of Messengers, who update their opinion quite rarely and integrate information only for a short duration. However, this duration is sufficient for them to process information and reach a consensus.

We also highlighted the transient and temporal aspects of collective behavior caused by the DMP. This perspective gives insight into understanding and studying the robustness of the performance against non-stationary behavior or dynamic conditions, particularly in scenarios where the initial conditions of the system are different than the expected stationary properties. For example, when the system starts with no Messengers and gradually increases the Messenger population to reach its expected value. Such analyses help engineer the system and guide designers to select parameters that are more robust against transient behaviors. Moreover, we simulated the model in various information distributions with both uni- and multi-modal shapes to assess the dependency of behavior on specific cases. The results showed negligible qualitative differences across different information distributions.

While only varying the DMP parameters and keeping the other parameters of the model constant has allowed for an in-depth exploration of the system, future research could expand on this by investigating the influence of the other parameters of the model. This includes aspects such as collective density, arena size, or information noise. Also, investigating the one-dimensional version, which resembles classical opinion dynamics more closely, could provide valuable insights into a range of related issues in the field.

## 4 Methods

In the following subsections, we describe how we used an agent-based modeling approach to simulate the opinion dynamics of collectives with homophily in space. Then, we provide the metrics we used to evaluate the behavior and performance of the collective.

### 4.1 Model

Our baseline model simulates Exploiter agents, whose behavior follows two chief components, conformity and homophily. Thereafter, we introduce a new behavior role for agents, called Messenger. To decide which role to take, agents use DMP, a stochastic Markov process. In the following, we elaborate on our modeling of agents' behavior.

#### 4.1.1 Conformity as an opinion-updating rule

Agents are interconnected via the communication network and continuously exchange information with their local neighbors. Conformity, as a form of social influence, causes individuals to change their opinions to get closer to each other when they are exposed to their social neighbors' opinions. Therefore, conformity poses a constraint on the opinion of agents in the network. Following the DeGroot naive social learning model [11], this dynamic constraint describes how agents modify their opinions based on the information they receive from their neighbors. The updating rule of the opinion is formulated as a weighted average of three different components [41]. These three sources of information influencing each agent's opinion are individual memory of opinion ( $z_i^t \in \mathbb{R}$ ), environmental signal ( $s_i^t$ ), and social signal

$(\sum_{j \in \mathbb{N}_i} z_j^t)$  which are described in:

$$z_i^{t+1} = \alpha z_i^t + \frac{1 - \alpha}{1 + N_i} \left( s_i^t + \sum_{j \in \mathbb{N}_i} z_j^t \right). \quad (1)$$

The weighted average of these three components shapes the opinion of each individual. The weights are defined explicitly by the self-weight ( $\alpha$ ), and implicitly by the size of the  $i$ -th agent's neighbor set  $N_i = |\mathbb{N}_i|$ . The scalar environmental signal  $s_i^t$  is derived from a function  $f$  that represents the information landscape. This function  $f$  maps the position of agents in a two-dimensional space  $\mathbb{R}^2$  to a scalar value in  $\mathbb{R}$ , i.e.,  $f : \mathbb{R}^2 \rightarrow \mathbb{R}$ .

#### 4.1.2 Homophily as a motion constraint

In our model, agents are not fixed in the information landscape and they actively move in it to search for sources of information matching their opinion. Their movement is determined by the information they receive from the environment and their local neighbors, therefore their neighbors can indirectly make them move in space. This adds to the formation of opinions and drives more complex collective motions in space. To model this, we used homophily as a mechanism for agents to change their position in space so that the information they receive fits better with the average of their local neighbors. This movement is considered an extra step to increase the consensus and happens in the space domain. To implement this movement, we defined an objective function based on the difference of two signals: what comes from the environment, and what the local neighbors agree upon. The difference makes a potential-like function in space that can push agents to specific points where the difference is minimal. So, homophily is an effort to minimize the difference between two values as dissonance value:

$$d_i^t = \frac{1}{2} (s_i^t - z_{\text{loc},i}^t)^2. \quad (2)$$

With the local collective average that agent  $i$  observes being defined as  $z_{\text{loc},i} = \sum_{i=1}^{N_i} z_i / N_i$ . Agents need to optimize this objective function to satisfy the homophily constraint. To implement it in a distributed way, we applied a minimal sample-wise pseudo-gradient descent (same as in [41]), where agents use the differentiation of the samples they measure, as an approximation of the gradient. We used this optimization method since it is independent of the gradient of the objective function, and requires minimal capabilities, being applicable for engineering cases as we showed in [17]. Agents constantly evaluate the dissonance value while they move in space. To approximate the slope of the function at position  $\mathbf{s}_i^t = [x_i^t, y_i^t]^T$ , agents calculate the differentiation of the objective function over the step they took in the last time step. A decaying memory (weighted by  $\beta$ ) of this differentiation smoothens the approximation of the gradient:

$$\nabla_{\mathbf{s}} d_i^t = \beta \nabla_{\mathbf{s}} d_i^{t-1} + (1 - \beta) \left[ \frac{\partial d_i^t}{\partial x_i^t}, \frac{\partial d_i^t}{\partial y_i^t} \right]^T, \quad (3)$$

$$\frac{\partial d_i^t}{\partial x_i^t} \approx \frac{\Delta d_i^t}{x_i^t - x_i^{t-1}}, \quad \frac{\partial d_i^t}{\partial y_i^t} \approx \frac{\Delta d_i^t}{y_i^t - y_i^{t-1}}. \quad (4)$$

To add randomness to the movement of agents, we define a vector along this gradient in addition to a random walk component:

$$\boldsymbol{\lambda}_i^t = (1 - r_\lambda) \frac{-\nabla_s d_i^t}{\|\nabla_s d_i^t\|} + r_\lambda \boldsymbol{\eta}_i^t, \quad (5)$$

in which,  $r_\lambda$  and  $\boldsymbol{\eta}_i^t$  are the weight of the random walk, and a vector of uniform random variables in  $[-1, +1]$ , respectively. Based on this vector, agents take a step ( $\mathbf{w}$ ) with a fixed size  $w$ :

$$\mathbf{w} = w \frac{\boldsymbol{\lambda}_i^t}{\|\boldsymbol{\lambda}_i^t\|}, \quad (6)$$

In cases where an agent does not have any neighbors, the movement follows only the random walk. Also, solitary agents will continue walking randomly and update their opinions based on the environmental information until they encounter a neighbor.

## 4.2 New Behavior: Data Ferrying by Messengers

A potential solution to tackle over-exploitation and the formation of echo chambers due to the limited communication range is to restore the effective connectivity of the network, especially the inter-cluster links of the network. The information can flow across clusters with different opinions and diffuse throughout the network. From an engineering perspective, a trivial solution would be to scale the problem by increasing the communication range, hence pushing the system to higher connectivity regimes. Improving the hardware, if possible, comes with physical constraints and increases the cost of the designed system. However, by harnessing the mobility of the agents, an alternative solution is to transmit information via the physical movement of agents carrying it in space. This way, different clusters can exchange information over distances that are possibly much larger than the communication range. To achieve this, we introduce a new, so-called ‘‘Messenger’’ state for agents to transfer the information as they move in space. A Messenger can be seen as embodied data that moves around in space and shares the information with its local neighbors that it encounters on its way. This is a similar concept as Zealots or stubborn agents who do not change their opinions [43–45]. A Messenger moves in space and establishes new links with other agents. The Messenger state should have the following fundamental properties:

- A Messenger does not modify its opinion while carrying it around. The value of the data is set to the last opinion of the agent, before becoming a Messenger.
- A Messenger moves randomly and independently of environment measurements, the data it carries, or social signals received from its local neighbors.
- A Messenger continually shares its fixed opinion value with the others it encounters.

In other words, a Messenger agent establishes long-distance uni-directional links by broadcasting its opinion to local neighbors while moving randomly in space. A Messenger migrating by chance from one cluster to another resembles and implements long, weak ties in a dynamic spatial network [46]. A Messenger state is in contrast with the ‘‘Exploiter’’ state. An Exploiter *integrates* the information following the model we explained in the previous subsections, whereas a Messenger behaves as a moving memory of *information*. A receiver agent, whether Messenger or Exploiter, does not distinguish the transmitter of the incoming



information. An Exploiter receives social information from other Exploiters or Messengers and integrates it regardless of its source. In contrast, Messengers do not process the incoming information and hence are regarded as *information*; information about the history of opinions. In this regard, a Messenger provides a link to the history of its opinion or, in some cases, the opinion of its cluster.

Agents can switch back and forth between the two states. When an Exploiter turns into a Messenger, it carries its latest opinion. If this opinion was the local consensus, then the data represents the opinion of the cluster. Similarly, a Messenger can switch back to an Exploiter state. In that case, the agent forgets its data and replaces it with the current information it receives from the environment. This causes another functional benefit of Messengers which is increased exploration. The challenge is to define a mechanism for agents to switch their states. In the following subsection, we propose a simple switching mechanism in a fully decentralized manner based on the DMP. First, we briefly review the properties of DMPs.

### 4.3 Dichotomous Markov Process (DMP)

This specific type of Markov process provides a probabilistic mechanism for switching between two contrasting states, Exploiter and Messenger in our case. The ability to implement it in a decentralized way is an essential feature in our scenario. We implement the DMP such that each agent  $i$  at time step  $t$  either remains in its current state or switches to the other state. An agent in an Exploiter state switches to Messenger with a transition probability  $p_M$ , and vice versa with probability  $p_E$ , per time step. The complement of each transition probability ( $1 - p_M$ , and  $1 - p_E$ ) determines the probability of remaining in the current state. The process is illustrated as a state machine in Fig. 9. We implement the process in a discrete-time domain, and we use  $\Delta t = 1$ . Hence, we formulate the DMP in terms of transition probabilities instead of transition rates [42]. The properties of the behavior for each agent are defined by the two parameters  $p_M$ ,  $p_E$ . Two properties that are of interest in this paper are the sojourn time and the expected ratio of Messengers. Assuming the stationary process, the sojourn time [47], denoted as the time between two consecutive switches, for each of the states is defined as follows:

$$\mathbb{E}[\tau_M] = \frac{1}{p_E}, \quad \mathbb{E}[\tau_E] = \frac{1}{p_M}.$$

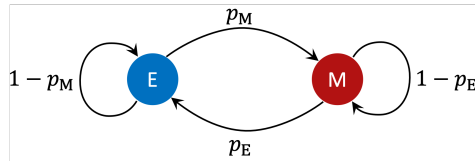


**Fig. 9:** DMP state-machine diagram illustrating how each individual switches its state between Exploiter and Messenger.

Then, we define sojourn time ( $\tau_S$ ), the average time steps spent in either of the states before switching, as the average of the two sojourn times:

$$\mathbb{E}[\tau_S] = \frac{1}{2} \frac{p_E + p_M}{p_E p_M}. \quad (7)$$

In this paper, we assume all agents have identical parameters. Nonetheless, due to the stochastic nature of the process, the collective properties are probabilistic. Therefore, we provide the relation between the *expected* values of the collective properties and the parameters of the DMP. The ratio of times agents spend in either of the states determines the ratio of Messengers (and Exploiters) in the collective at a given time step. The expected steady-state Messenger ratio ( $m$ ) follows the equation below:

$$\mathbb{E}[m] = \mathbb{E}\left[\frac{M}{N}\right] = \frac{p_M}{p_E + p_M}. \quad (8)$$

## 4.4 Metrics and Setup

Here we define evaluation metrics to benchmark the collective performance. We have metrics of two types: the first type evaluates the collective in the opinion domain, i.e. by using the internal opinion of each agent; while the second does not require access to the internal state of the agents, but their position in the physical space. By quantifying the precision of the collective opinion, the spatial arrangement of agents in space, and the connectivity of the communication network, these metrics capture all relevant aspects of the collective performance. To show how Messengers change the performance of the collective, we normalize the absolute metrics to that of the *baseline* setup, where there is no Messenger in the collective. Please note that in our finite size stochastic simulations, the expected ratio of Messengers for the bottom right corner of the parameter space is  $\mathbb{E}[m] < 10^{-8}$ , which validates the zero-Messenger assumption. We refer to these metrics as normalized metrics.

### 4.4.1 Precision Error

Since the objective of the problem is similar to [41], we use the same metrics and refer readers to the original paper for further details. We decomposed the total accuracy error into trueness and precision errors. In this paper, we assume that the initial distribution of agents is diverse enough and the trueness error (collective bias) is negligible ( $z_{\text{col}} \approx z_{\text{gt}}$ ). Hence, we only report the precision error as it contains the necessary information about achieving consensus. We obtain the *opinion* precision error as the variance of the opinions with respect to the collective (average) opinion ( $z_{\text{col}} = \sum_{i=1}^N z_i / N$ ) as following:

$$E_P^O = \frac{1}{N} \sum_{i=1}^N (z_i - z_{\text{col}})^2. \quad (9)$$

To show the precision of the spatial positioning of the collective, i.e. spatial consensus, we use the same metric and take the position of agents instead. This metric directly quantifies the performance in terms of contour capturing [17]. The precision error in the *space* domain

measures how close are agents to the collective average with regard to the information distribution. We distinguish the two domains by a superscript and define the precision error in the *space* domain as:

$$E_p^S = \frac{1}{N} \sum_{i=1}^N (s_i - s_{\text{col}})^2. \quad (10)$$

#### 4.4.2 Number of Clusters

Another metric that measures the cohesion of the agents in the physical space, particularly considering their communication network, is the number of connected components they form in their network. To count the clusters, we find connected components based on the communication range of agents and assign adjacent agents to the same cluster. We count how many clusters are present in the network.

### 4.5 Simulation Configuration

As an extension of our previous work [41], we used the same parameters, except for the communication range. To put the system in a regime where echo chambers can potentially emerge, we set the communication range to  $r_{\text{comm}} = 0.1$ . This is similar to the configuration of Kilobots [48], a robotic platform used to study collective behaviors, which we used to implement the baseline setup in a real-world setting [17]. Also, we distributed the probabilities ( $p_E, p_M$ ) exponentially, same as in Fig. 4. This way, we can reveal a wide spectrum of the DMP dynamics on various scales. The results that we report are the average of 24 independent Monte-Carlo simulations. Otherwise noted, we used the parameters of the model as reported in Table 1.

Name	Description	Value
N	Number of Agents	100
A	Arena Size	$2 \times 2$
$r_{\text{comm}}$	Communication Range	0.15
w	Walking Step Size	0.002
$t_f$	Simulation Time Step Duration	50,000
$\sigma$	Measurement Noise	0.001
$\delta_t$	Integration Interval	1
$\alpha$	Self-weight on Opinion Memory	0.99
$\beta$	Decaying Factor for Gradient Descent	0.9
$p_E$	Probability of Switching to Messenger State	$\exp\{-20 : -2\}$
$p_M$	Probability of Switching to Exploiter State	$\exp\{-20 : -2\}$

**Table 1:** Simulation Parameters

## 5 Data Availability

The datasets generated and analyzed during the current study will be available online.

## 6 Code Availability

The underlying code for this study is available in the GitHub repository and can be accessed via this link <https://github.com/mohsen-raoufi/messengers>.

## Acknowledgments

This study was funded by the Deutsche Forschungsgemeinschaft (DFG, German Research Foundation) under Germany's Excellence Strategy – EXC 2002/1 “Science of Intelligence” – project number 390523135. The funder played no role in study design, data collection, analysis and interpretation of data, or the writing of this manuscript.

## References

- [1] Bonabeau, E., Dorigo, M. & Theraulaz, G. *Swarm intelligence: from natural to artificial systems* (Oxford university press, 1999).
- [2] Krause, J., Ruxton, G. D. & Krause, S. Swarm intelligence in animals and humans. *Trends in ecology & evolution* **25**, 28–34 (2010).
- [3] Leonard, N. E. & Levin, S. A. Collective intelligence as a public good. *Collective Intelligence* **1**, 26339137221083293 (2022).
- [4] Galton, F. Vox populi (the wisdom of crowds). *Nature* **75**, 450–451 (1907).
- [5] Surowiecki, J. *The wisdom of crowds* (Anchor, 2005).
- [6] Budescu, D. V. & Chen, E. Identifying expertise to extract the wisdom of crowds. *Management science* **61**, 267–280 (2015).
- [7] Golub, B. & Jackson, M. O. Naive learning in social networks and the wisdom of crowds. *American Economic Journal: Microeconomics* **2**, 112–49 (2010).
- [8] Prelec, D., Seung, H. S. & McCoy, J. A solution to the single-question crowd wisdom problem. *Nature* **541**, 532–535 (2017).
- [9] Da, Z. & Huang, X. Harnessing the wisdom of crowds. *Management Science* **66**, 1847–1867 (2020).
- [10] Winklmayr, C., Kao, A. B., Bak-Coleman, J. B. & Romanczuk, P. The wisdom of stalemates: consensus and clustering as filtering mechanisms for improving collective accuracy. *Proceedings of the Royal Society B* **287**, 20201802 (2020).
- [11] DeGroot, M. H. Reaching a consensus. *Journal of the American Statistical Association* **69**, 118–121 (1974).
- [12] Olfati-Saber, R., Fax, J. A. & Murray, R. M. Consensus and cooperation in networked multi-agent systems. *Proceedings of the IEEE* **95**, 215–233 (2007).

- [13] Xia, H., Wang, H. & Xuan, Z. Opinion dynamics: A multidisciplinary review and perspective on future research. *International Journal of Knowledge and Systems Science (IJKSS)* **2**, 72–91 (2011).
- [14] Lorenz, J. & Neumann, M. Opinion dynamics and collective decisions. *Advances in Complex Systems* **21**, 1802002 (2018).
- [15] Xiao, L., Boyd, S. & Lall, S. N/A (ed.) *A scheme for robust distributed sensor fusion based on average consensus*. (ed.N/A) *IPSN 2005. Fourth International Symposium on Information Processing in Sensor Networks, 2005.*, 63–70 (IEEE, 2005).
- [16] Leonard, N. E. *et al.* Collective motion, sensor networks, and ocean sampling. *Proceedings of the IEEE* **95**, 48–74 (2007).
- [17] Raoufi, M., Romanczuk, P. & Hamann, H. N/A (ed.) *Estimation of continuous environments by robot swarms: Correlated networks and decision-making*. (ed.N/A) *2023 IEEE International Conference on Robotics and Automation (ICRA)*, 5486–5492 (2023).
- [18] Zha, Q. *et al.* Opinion dynamics in finance and business: a literature review and research opportunities. *Financial Innovation* **6**, 1–22 (2020).
- [19] Maia, H. P., Ferreira, S. C. & Martins, M. L. Adaptive network approach for emergence of societal bubbles. *Physica A: Statistical Mechanics and its Applications* **572**, 125588 (2021).
- [20] Castellano, C., Fortunato, S. & Loreto, V. Statistical physics of social dynamics. *Reviews of modern physics* **81**, 591 (2009).
- [21] Liggett, T. M. *Stochastic Interacting Systems: Contact, Voter and Exclusion Processes* Vol. 324 (Springer Science & Business Media, 1999).
- [22] Hegselmann, R. & Krause, U. Opinion dynamics and bounded confidence models, analysis and simulation. *Journal of Artificial Societies and Social Simulation* **5** (2002).
- [23] Sirocchi, C. & Bogliolo, A. Topological network features determine convergence rate of distributed average algorithms. *Scientific Reports* **12**, 21831 (2022).
- [24] Galesic, M. *et al.* Beyond collective intelligence: Collective adaptation. *Journal of the Royal Society interface* **20**, 20220736 (2023).
- [25] Fisher, D. N. & Pinter-Wollman, N. Using multilayer network analysis to explore the temporal dynamics of collective behavior. *Current zoology* **67**, 71–80 (2021).
- [26] McPherson, M., Smith-Lovin, L. & Cook, J. M. Birds of a feather: Homophily in social networks. *Annual review of sociology* **27**, 415–444 (2001).
- [27] Karimi, F., Génois, M., Wagner, C., Singer, P. & Strohmaier, M. Homophily influences ranking of minorities in social networks. *Scientific reports* **8**, 11077 (2018).

- [28] Lee, E. *et al.* Homophily and minority-group size explain perception biases in social networks. *Nature human behaviour* **3**, 1078–1087 (2019).
- [29] Del Vicario, M. *et al.* The spreading of misinformation online. *Proceedings of the National Academy of Sciences* **113**, 554–559 (2016).
- [30] Bakshy, E., Messing, S. & Adamic, L. A. Exposure to ideologically diverse news and opinion on facebook. *Science* **348**, 1130–1132 (2015).
- [31] Lovato, J. *et al.* Diverse misinformation: impacts of human biases on detection of deepfakes on networks. *npj Complexity* **1**, 5 (2024).
- [32] Törnberg, P. Echo chambers and viral misinformation: Modeling fake news as complex contagion. *PLoS one* **13**, e0203958 (2018).
- [33] Stein, J., Keuschnigg, M. & van de Rijt, A. Network segregation and the propagation of misinformation. *Scientific Reports* **13**, 917 (2023).
- [34] Mocanu, D., Rossi, L., Zhang, Q., Karsai, M. & Quattrociocchi, W. Collective attention in the age of (mis) information. *Computers in Human Behavior* **51**, 1198–1204 (2015).
- [35] Levy, G. & Razin, R. Echo chambers and their effects on economic and political outcomes. *Annual Review of Economics* **11**, 303–328 (2019).
- [36] Holme, P. & Newman, M. E. Nonequilibrium phase transition in the coevolution of networks and opinions. *Physical Review E* **74**, 056108 (2006).
- [37] Bullock, S. & Sayama, H. N/A (ed.) *Agent heterogeneity mediates extremism in an adaptive social network model*. (ed.N/A) *Proceedings of the Artificial Life Conference 2023 (ALIFE 2023)* (Massachusetts Institute of Technology (MIT) Press, 2023).
- [38] Zanette, D. H. & Gil, S. Opinion spreading and agent segregation on evolving networks. *Physica D: Nonlinear Phenomena* **224**, 156–165 (2006).
- [39] Mengers, V., Raoufi, M., Brock, O., Hamann, H. & Romanczuk, P. Leveraging uncertainty in collective opinion dynamics with heterogeneity. *arXiv preprint arXiv:2402.03354* (2024).
- [40] Wu, Z. *et al.* Mixed Opinion Dynamics Based on DeGroot Model and Hegselmann–Krause Model in Social Networks. *IEEE Trans. Syst. Man Cybern, Syst.* **53**, 296–308 (2023). URL <https://ieeexplore.ieee.org/document/9788051/>.
- [41] Raoufi, M., Hamann, H. & Romanczuk, P. N/A (ed.) *Speed-vs-accuracy tradeoff in collective estimation: An adaptive exploration-exploitation case*. (ed.N/A) *2021 International Symposium on Multi-Robot and Multi-Agent Systems (MRS)*, 47–55 (2021).

- [42] Bena, I. Dichotomous Markov noise: exact results for out-of-equilibrium systems. *International Journal of Modern Physics B* **20**, 2825–2888 (2006).
- [43] Galam, S. & Jacobs, F. The role of inflexible minorities in the breaking of democratic opinion dynamics. *Physica A: Statistical Mechanics and its Applications* **381**, 366–376 (2007).
- [44] Mobilia, M., Petersen, A. & Redner, S. On the role of zealotry in the voter model. *Journal of Statistical Mechanics: Theory and Experiment* **2007**, P08029 (2007).
- [45] Verma, G., Swami, A. & Chan, K. The impact of competing zealots on opinion dynamics. *Physica A: Statistical Mechanics and its Applications* **395**, 310–331 (2014).
- [46] Granovetter, M. S. The strength of weak ties. *American journal of sociology* **78**, 1360–1380 (1973).
- [47] Rubino, G. & Sericola, B. Sojourn times in finite markov processes. *Journal of Applied Probability* **26**, 744–756 (1989).
- [48] Rubenstein, M., Ahler, C. & Nagpal, R. N/A (ed.) *Kilobot: A low cost scalable robot system for collective behaviors*. (ed.N/A) *2012 IEEE International Conference on Robotics and Automation*, 3293–3298 (IEEE, 2012).



## Appendix

### Relaxation Time of the DMP

An important property of the DMP to consider for studying the transient behavior of Markov Processes is relaxation time ( $\tau_c$ ). The relaxation time is the time that it takes for the system to converge to its stationary state [42]:

$$\tau_c = \frac{1}{p_E + p_M}.$$

Fig. 10 illustrates how the relaxation time is determined by transition probabilities. This figure supplements Fig. 7 and clarifies the change in the optimal lower-left part of the parameter space.

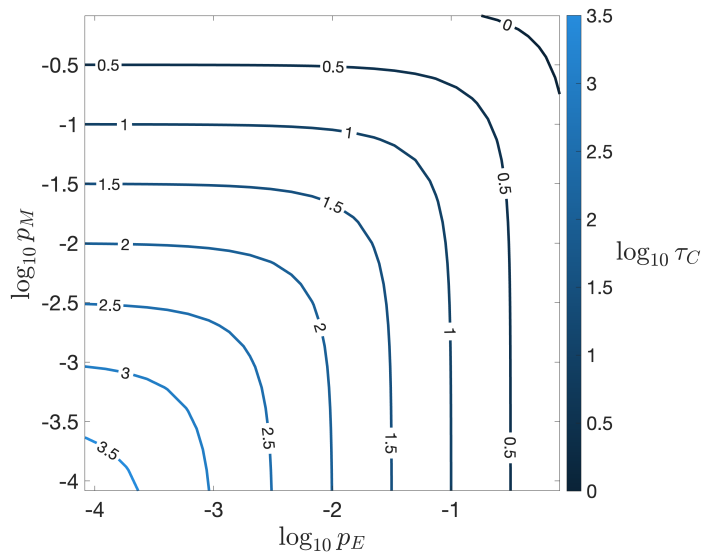


**Fig. 10:** Relaxation time of the DMP

### Time-Development of Opinions

The time development of agents' opinions and positions illustrates how collective forms over time. It also demonstrates that the two dimensions of opinion and position are separate, especially for Messengers whose opinions are independent of their position in space. In Fig. 11, we showed how opinions and positions of agents evolve over time for different pairs of DMP parameters. We used the radial mapping of agents' positions to convert the 2D positions into a one-dimensional variable.

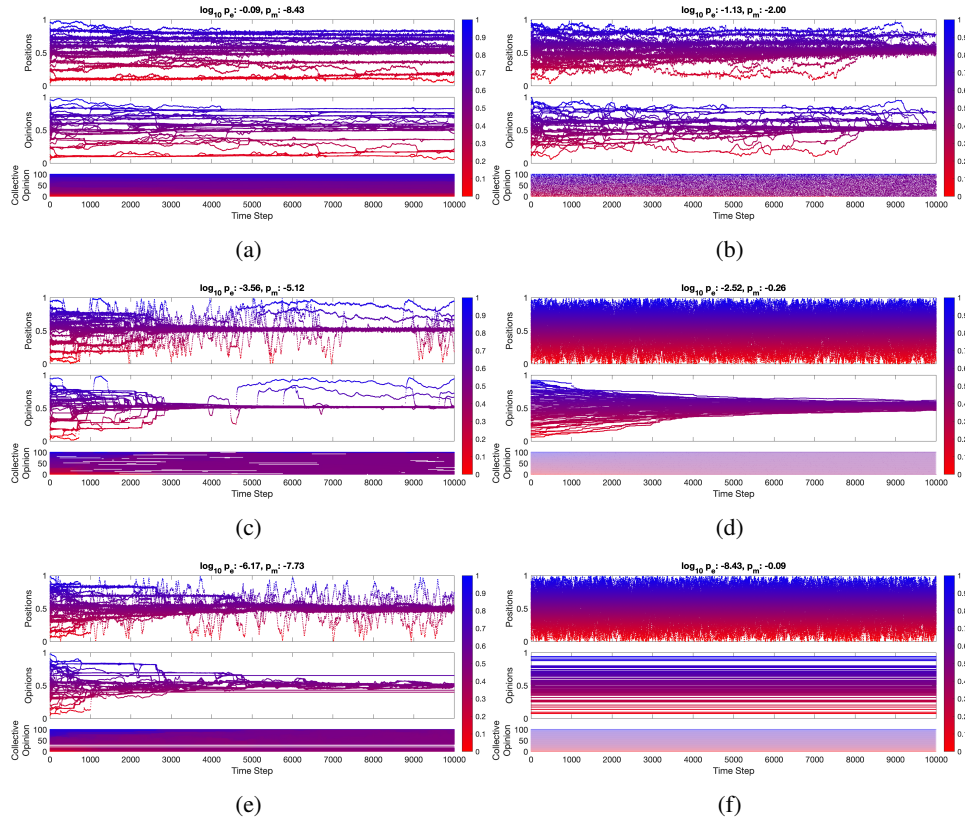


**Fig. 11:** Temporal development of opinions and positions for different DMP parameters. The first and second rows show the position and opinion of agents, respectively. The third rows illustrate the distribution of collective opinion over time with Messengers as white dots. a) Too many Exploiters (R1), b) a few fast-switching Messengers (R2-b), c) a few slow-switching Messengers (R2), d) many fast-switching Messengers (R2-c), e) a few specialized Messengers with no switching, and e) all Messengers (R3).

## One-dimensional Information landscape

Our results for a similar system in one-dimensional opinion space confirm our results for the 2D system. Among the few modifications needed to fit the model to the 1D scenario, updating the random walk had a significant impact on the performance. We know that for random walking agents, the probability of encountering another agent drops significantly with the dimension size. This can also open new doors to investigating the performance of the Messengers in high-dimensional space. The development of agents' opinions, when the information landscape is one-dimensional, resembles the classic opinion dynamics with bounded confidence, see Fig. 12.

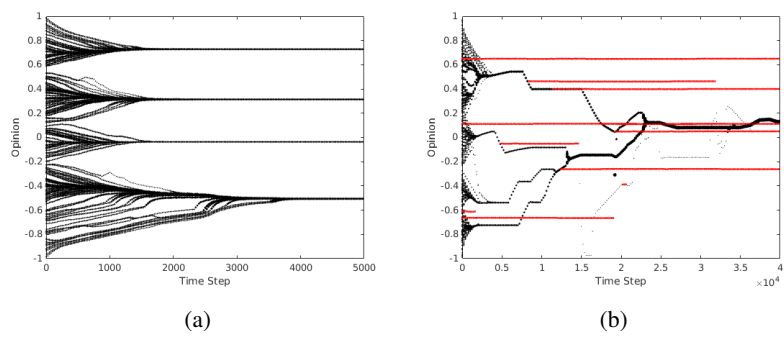


**Fig. 12:** Temporal development of opinions for 1D information space, a) echo chambers emerge without Messengers, b) Messengers bring consensus back to the collective.